# Digital Forensics for the Health Sciences:

## Applications in Practice and Research

Andriani Daskalaki
*Max Planck Institute for Molecular Genetics, Germany*

Medical Information Science REFERENCE

MEDICAL INFORMATION SCIENCE REFERENCE

Hershey · New York

Senior Editorial Director: Kristin Klinger
Director of Book Publications: Julia Mosemann
Editorial Director: Lindsay Johnston
Acquisitions Editor: Erika Carter
Development Editor: Joel Gamon
Production Coordinator: Jamie Snavely
Typesetters: Keith Glazewski & Natalie Pronio
Cover Design: Nick Newcomer

Published in the United States of America by
Medical Information Science Reference (an imprint of IGI Global)
701 E. Chocolate Avenue
Hershey PA 17033
Tel: 717-533-8845
Fax: 717-533-8661
E-mail: cust@igi-global.com
Web site: http://www.igi-global.com



Library of Congress Cataloging-in-Publication Data

Digital forensics for the health sciences : applications in practice and research / Andriani Daskalaki, editor.
p. cm.
Summary: "This book discusses current applications of digital forensics in health sciences as well as the latest research in this area, with coverage in basic concepts, best practices, common techniques, investigative challenges and, most importantly, the major limitations of current tools and approaches"-- Provided by publisher.
Includes bibliographical references and index.
ISBN 978-1-60960-483-7 (hardcover) -- ISBN 978-1-60960-484-4 (ebook) 1. Radiography, Medical--Digital techniques. 2. Medical jurisprudence--Data processing. I. Daskalaki, Andriani, 1966-
RC78.7.D35D52 2011
616.07'572--dc22
2010054472

British Cataloguing in Publication Data
A Cataloguing in Publication record for this book is available from the British Library.

# Chapter 5
# Facial Reconstruction as a Regression Problem

**Maxime Berar**
*Université de Rouen, France*

**Michel Desvignes**
*GIPSA-LAB, France*

**Françoise Tilotta**
*Université Paris Descartes, France*

**Marek Bucki**
*Laboratoire TIMC-IMAG, France*

**Joan A. Glaunès**
*Université Paris Descartes, France*

**Yohan Payan**
*Laboratoire TIMC-IMAG, France*

**Yves Rozenholc**
*Université Paris Descartes, France*

## ABSTRACT

*This chapter presents a computer-assisted method for facial reconstruction. This method provides an estimation of the facial outlook associated with unidentified skeletal remains. Current computer-assisted methods using a statistical framework rely on a common set of points extracted form the bone and soft-tissue surfaces. Facial reconstruction then attempts to predict the position of the soft-tissue surface points knowing the positions of the bone surface points. This chapter proposes to use linear latent variable regression methods for the prediction (such as Principal Component Regression or Latent Root Root Regression) and to compare the results obtained to those given by the use of statistical shape models. In conjunction, the influence of the number of skull landmarks used was evaluated. Anatomical skull landmarks are completed iteratively by points located upon geodesics linking the anatomical landmarks. They enable artificial augmentation of the number of skull points. Facial landmarks are obtained using a mesh-matching algorithm between a common reference mesh and the individual soft-tissue surface meshes. The proposed method is validated in terms of accuracy, based on a leave-one-out cross-validation test applied on a homogeneous database. Accuracy measures are obtained by computing the distance between the reconstruction and the ground truth. Finally, these results are discussed in regard to current computer-assisted facial reconstruction techniques, including deformation based techniques.*

DOI: 10.4018/978-1-60960-483-7.ch005

## INTRODUCTION

In forensic medicine, craniofacial reconstruction refers to any process that aims to recover the morphology of the face from skull observation (Wilkinson, 2005). Otherwise known as facial approximation, it is usually considered when confronted with an unrecognisable corpse and when no other identification evidence is available. This reconstruction may hopefully provide a route to a positive identification. Forensic facial reconstruction is more of a tool for recognition, than a method of identification [Wilkinson]: it aims to provide a list of names from which the individual may be identified by accepted methods of identification. Since its conception in the 19th century, two schools of thought have developed in the field. To answer the question "will only one face be produced from each skull", facial "approximators" claim that many facial variations from the same skull may be produced, whereas practitioners of the other school of thought attempt to characterised the individual skull morphology to make the individual recognisable. In recent years, computer-assisted techniques have been developed following the evolution of medical imaging and computer science. As presented in the surveys in Buzug (2006), Clemens (2005), DeGreef (2005), and Wilkinson (2005), computerised approaches are now available with reduced performance timeline and operator subjectivity.

The first machine-aided methods were inspired by manual methods. Manual reconstruction follows four basic steps, (according to Helmer, 2003): Examination of the Skull, Development of a Reconstruction Plan, Practical Sculpturing and Mask Design. Translated into a computer-assisted framework, these steps are according to Buzug (2006): Computed Tomography Scan of the skull, Matching of a Soft Tissue Template, Warping of Template onto Skull Find and Texture Mapping/ Virtual Make-Up. The first step aims to extract structural characteristics: for example key skull dimension for manual methods or crest-lines (Quatrehomme, 1997) for computer assisted ones. Another example is the location, automatically or by an expert of cephalometric points. Skulls and facial surfaces have been collected using a variety of 2- and 3-D methods such as photography (Stratomeier, 2005), video (Evison 1996), laser scanning (Claes, 2006), magnetic resonance imaging (Paysan, 2009; Mang, 2006; Michael, 1996), holography (Hirsch, 2005; Hering, 2003), mobile digital ultrasound scanner (Claes, 2006), computed tomography scanning (Jones, 2001; Bérar, 2006; Tu, 2007) .The second step consists in compiling all the data obtained during the investigation and listing soft-tissue depths for specified points of the face in accordance with the individual 's gender and type of constitution. This is the equivalent of the "Matching of a Soft Tissue Template" step, which aims at identifying an appropriate soft-tissue template from a database or inject in the model the estimated age, body mass index, gender or ancestry.

The third step is either the modeling of the muscles using wax, followed by the embedding of eye glass, then by the modeling of the nose, mouth and eyelids, ... or the deformation of the face template in order to fit the set of virtual dowels placed on the virtual skull on given landmarks. Interactive correction of individual parts of the face was usually necessary in the computerized reconstruction and, similarly, the wax face is reworked to achieve a natural appearance. The last step consists in achieving of a natural-looking face. In summary, the first machine-aided techniques fitted a skin surface mask to a set of interactively placed virtual dowels on the digitized model of the remains (Evenhouse, 1992; Vanezis, 2000; Shahrom, 1996). These techniques did not try to learn the relationships between bone surfaces and soft-tissue surfaces but to use the relationships described in soft-tissue depth tables (Rhine, 1980, 1984). Moreover, skilled operators were necessary in the choice of facial templates, features or sculptural distortions, thus creating a depen-

dency on the practitioner training and subjectivity (Wilkinson, 2005).

Later techniques have moved away from the manual techniques and use the relationships between soft-tissue and bone surfaces. Two kinds of methods can be distinguished based on the representation of the bone and soft-tissue volumes. The first type of techniques aims to keep the continuous nature of the skull and soft-tissue surfaces. Estimates of the face are obtained by applying deformations of the space to couples of known bone and soft tissue surfaces, called reference surfaces. These deformations are learned between the surface of the dry skull and the surfaces of the reference skulls and then applied on the surfaces of the reference faces. They can be parametric (e-g B-splines) (Kermi 2007; Vandermeulen 2006), implicit using variational methods (Mang, 2006; Mang, 2007) or volumetric (Nelson, 1998; Quatrehomme, 1997). Depending on the method, the final estimated face can be either the deformed face whose reference skull is the nearest of the dry skull (Nelson, 1998; Quatrehomme, 19970 or a combination of all the deformed soft-tissue surfaces (Vandermeulen, 2006; Tu, 2007). Here, the relationships between the surfaces are not learned but conserved through the deformation fields. To a single dry skull corresponds as many deformed faces as subjects in the database, and all the combinations possible between them (the more common combination being the mean). The generic deformations applied to the templates are not face-specific, but only ''smooth'' in a mathematical sense. No problem arises when the differences between the model and the target skull-based surfaces are small. However, if these differences are relatively large, the required deformation will be more pronounced, resulting in a possibly unrealistic or implausible facial reconstruction.

The second type of approaches chooses to represent individuals using a common set of points, like soft-tissue depths were originally measured. As the position of the corresponding points for all the individuals can be summarised as variables in a table, the main idea is then to use statistics to decipher the relation between the skull and the soft-tissue. The common set of points can either be anatomical landmarks (Claes, 2006; Vanezis, 2000) or semi-landmarks located following a point correspondence procedure (Berar, 2006; Kähler, 2003: Paysan, 2009). Semi-landmarks are defined as points that do not have names but that match across all the samples of a data set under a reasonable model of deformation (Bookstein, 1997). Usually, a small set of anatomical landmarks is used to represent the bone surface whereas a larger set of points is used to represent the soft-tissue surface. The larger the set, the more this representation of the surface approaches a real surface. Apart from the practical constraint of the number of anatomical landmarks that an expert can define and extract, there is no justification of a chosen number of points used to represent the skull surface. Indeed, the information given by the position of skull anatomical landmarks is double. First, there is geometric information given by the coordinates of the points. Then, "anatomic" information is given by the measures of tissue thickness made on this points. This information is available for a limited number of points. However, the geometric information given by the position of the point can be completed by automatic methods of landmark extraction. The second part of the data analysis framework consists in learning the relationships between the soft-tissue variables and the bone variables. In current techniques, a linear model of the common variability of the positions of the points is learned -following the works made in statistical atlas, medical or audiovisual speech- called a statistical shape model (Cootes, 1995). Either the variability of the points of the soft-tissue surface (Claes, 2006; Basso, 2005; Tu, 2007), or each set of points of each surface (Paysan, 2009), or a set containing the points of both surfaces (Berar, 2006; Mang, 2006) can be learned. Statistical shape models describe the shape as a mean shape and a set of linear variations around it. Each of these variations is controlled by the modes of the

model, and any individual can be described by a set of values of the variations modes, also called variability parameters. Statistical shape models are an attempt to characterized the individual skull morphology to make the individual recognizable by the value of the variability parameters. For facial reconstruction, the predicted soft-tissue surface will be the instance of the shape model the nearest to the measured skull landmarks or analogous face points, depending on which of those points are included in the model.

However, the prediction of the positions of the soft-tissue points knowing the positions of the set of skull landmarks is a regression problem. The skull points will then be considered as entries of a regression model and the face points will be considered as the outputs of the model. Several regression methods have been developed, some sharing the ideas behind the statistical shape models. Principal Component Regression will build a statistical shape model of the shape of the skull and use the variability parameters of the model, also known as latent variables, as predictors for the regression problem. Another example of a latent variable regression method is Latent Root regression (Gunst, 1976; Vigneau, 2002). Designed to take into account the presence of co-linearity in the variables, in our case the positions of the skull landmarks and of the face semi-landmarks, it shares the use of Principal Component Analysis (Joliff, 1986) like the statistical shape model and indeed builds a joint statistical shape model of all the points, bone and soft-tissue alike.

For all facial reconstruction methods, the assessment of the accuracy, reliability and reproducibility of the computer-based systems is of paramount importance. Practitioners have relied for a long time on examples of successful forensic cases or subjective assessment of resemblance. Databases of surfaces enable us to obtain quantitative measures of the proximity between the shape of the predicted and validation samples. However, as each database is different, so are each digitalization and point correspondence procedures. Comparison of methods is therefore difficult and the quantitative measures of the proximity of surfaces do not translate well into a success rate for identification. Simplified face-pool tests have been used in order to estimate the identification success rate, established generating 2D images from the 3D models and showing them to human observers (Claes, 2006). In the same vein, correspondences between facial landmarks on the predicted surface and photographies can be researched (Tu 2007) as a short cut for a possible recognition.

In this chapter, we propose facial reconstruction techniques using linear regressions methods and compare the results obtained to those given by a statistical shape model. The deformation algorithm -used to build the database of soft-tissue meshes- provides one last facial reconstruction methodology, where the deformation field computed between the surface of the dry skull and a bone surface of the learning database will be applied to the corresponding face surface of the base to obtain a facial reconstruction. The same error criteria will be used to quantitatively compare all the obtained reconstructed faces. In conjunction, we interrogate the number of skull landmarks necessary. Basing our first experimentation on anatomical skull landmarks extracted by an expert, we will iteratively add supplementary mathematical skull landmarks following the point correspondence technique described in Wang (2000), which relies on the geodesic paths between the landmarks to define new landmarks. Regression methods will be used to predict the new points given by each iteration and those results compared to those of the facial reconstruction methods.

The chapter is organized as follows. The material and method are presented in a first section, which presents the material on which this study has been done. The following sections focus on resolving the point correspondence problem, describing the two methods used to obtain the two subject-shared descriptions of the bone and soft-tissue surfaces. Next, statistical methods are

discussed: the building and use of a statistical shape model, the Principal Component Regression and the multivariate Latent Root Regression method. Following this, the results obtained by the different models are shown and the influence of the number of skull landmarks and of the statistical method chosen is discussed.

## MATERIAL AND METHODS

This study was performed using whole head and skull surface meshes extracted from whole head CT scanners acquired for a project on facial reconstruction of University Paris Descartes. In the framework of this study, we focus on a group of 47 women aged from 20 to 40 years. Soft-tissue and bone surface meshes have been obtained following mathematical and computational processes described in Tilotta (2009). Anatomical skull landmarks were also manually located on each CT Scan according to classical methods of physical anthropology (13 midpoints and two sets of 13 lateral points). In order to artificially augment the size of the database, the entries of the database will consist of left or right halves of each surface meshes. The skull and the face do not have symmetric shapes, but the relationships between these face and skull shapes do not depend on the side of the head. The plan minimizing the distances to the anatomical midpoints has been chosen as an artificial boundary between the right and left part of the shapes.

The next step is to establish correspondences between the shapes of each subject in order to quantify the anatomical differences between subjects. It is a common step of the building of statistical shape models or of statistical atlases. According to the nature of the representation of the shape in the statistical model (surface, lines, points), this problem is reduced to a problem of correspondence between sets of points, lines or surfaces. Points correspondence procedures extract points which correspond to the same places on the different individuals. In consequences, each skull or face shape mesh shares the same mesh structure with the same number of vertices. For example, anatomical landmarks located by the expert establish a rough mesh for each subject with a shared structure between the subjects, whereas the variability of the position of the vertices reflects the anatomical characteristics of each subject. In the opposite, deforming a common mesh on all the subjects meshes will too share the structure of the deformed mesh. The location of the vertices of each deformed mesh will too reflect the anatomical characteristics of each subject. According to the point correspondence procedures used, the surfaces have to be cut in two at different steps of the procedures. The surfaces will be either cut following the boundary plan asa pre-processing step (soft-tissue surfaces) or cut as a post-processing step (bone surfaces).The automatically extracted points respect this symmetry constraint . The points shared between the left and right entries will be located on the boundary plan.

### Building Normalised Shapes: Point Correspondence Procedure for the Bone Surfaces

The anatomical landmarks located by the expert (Figure 1A) establish a first correspondence between the skulls. Following the scheme presented in Wang (2000), we define a set of triangular connections between these anatomical landmarks. For each pairs of connected points, we can extract a set of geodesic curbs between these points. Geodesics are defined to be the shortest path between points on the curved spaces of the shape surfaces (see Figure 1B). As the shape surface between two landmarks is different from a sphere, these geodesics are unique. At this step, a gross template of curbs on the surface between the landmarks is build. We then can define new landmarks as the midpoints of each geodesics and decompose each triangle into four new triangles. A more dense triangulation is then derived as seen Figure 1C.

*Figure 1. Iterative extraction of skull landmarks*

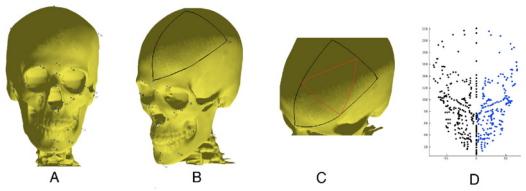


*Figure 2. Skull shape meshes generated for iteration 0 to 5*

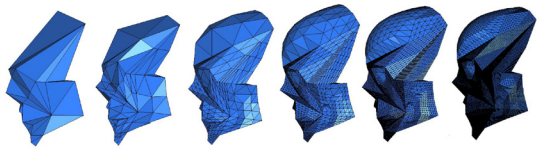

As the iterative process is repeated, the structure is refined to denser surface points and triangulation. The obtained structures form meshes, who share the same structure for each individual, and implicitly solve the point correspondence problem.

Moreover, the defined structure is symmetric: the two entries (left and right) of the database share a common substructure and set of midpoints (Figure 1D). Due to numerical instabilities, two methods of geodesics computation on surface meshes have been used: Surazhsky algorithm (Surazhsky, 2005) and Fast Marching Algorithm algorithm (Sethian, 1999), implemented by Peyre in the Geowave library. For two iterations of the procedure, it results in three sets of skull landmarks for each individual. A first set of points composed of the original landmarks: 13 midpoints and 13 lateral points. A second set composed of 54 points is added by the first iteration of the procedure (10 midpoints and 44 lateral points) and completed with 198 new landmarks by the second iteration (20 midpoints and 178 lateral points). The total number of points for each structure up to 5 iterations is shown Table 1.

Figure 2 shows skull meshes corresponding to successive iterations of the procedure. As more points are extracted, new levels of details are obtained especially in the superior part of the skull. A limit of this procedure occurs for very small length of one or more side of the triangles. In this case, the triangle degenerates into a point or a segment and subsequent iteration will extract all supplementary points in the same location. Moreover, as the surface encompassed by each triangles becomes smaller, the triangles become planar. All supplementary points are then situated on the same plane and the information given by the supplementary points is less useful.

*Table 1. Number of points by iteration of the procedure*

| Iteration | 0 | 1 | 2 | 3 | 4 | 5 |
|---|---|---|---|---|---|---|
| Number of points | 26 | 80 | 278 | 1034 | 3986 | 15650 |
| Mid-points | 13 | 23 | 43 | 83 | 163 | 323 |

## Building Normalised Shapes: Point Correspondence Procedure for the Soft-tissue Surfaces

For the soft-tissue surfaces, no landmarks are located. Moreover measures of tissue thickness are not provided: the number of skull landmarks corresponding to successive iterations of the former point correspondence procedure increases too much to allow manual measurements to be done. The quality of automatic extraction of tissue thickness on landmarks depends on the surface representation: the normal vectors on the surface meshes are sensitive to the triangulation used on the surfaces. Tissue thickness cannot be measured correctly and automatically on all possible landmarks (Tilotta, 2009).

Instead of facial points analogous to the anatomical skull points, we extract a set of semi-landmarks for each individuals neither really dense nor sparse. Working on the "half" surfaces previously defined, the point correspondence

procedure register a reference mesh (see Figure 3A) on the individual soft-tissue surface mesh (see Figure 3B) resulting on a deformed reference mesh (see Figure 3C). The registration is made computing an elastic deformation between the reference mesh and soft-tissue surface meshes of the database. The deformed meshes of each entry of the database have the same number of vertices (1741 for the mesh of an half face). The assumption of semi landmarks is then assumed: each vertex of the deformed reference meshes matches the same point for every individual. The 3D to 3D meshes matching algorithm used is a modified version of Szeliski algorithm (Szeliski, 1996). A first modification has been made to take into account the difference of density between the reference mesh and the high-density meshes of the soft-tissue surfaces. The second modification ensures that each vertex of the boundary of the deformed reference meshes is shared by the right and left meshes. The mesh used as the reference mesh correspond to the region of the face of head mesh modelled by F. Pighin (1999), where the density of vertices is greater in zones with high bending than in zones with low bending. This dissimilarity between the soft-tissue surface meshes and the reference meshes have consequences. The distances from the vertices of the deformed reference mesh to its associated soft-tissue surface mesh are null. However, the distances from the vertices of the soft-tissue mesh surface to the deformed reference mesh are not null.. The highest distances (superior to 3 mm) correspond to parts of the soft-tissue surfaces which do not have corresponding regions in the reference surface. Other distances correspond to regions like the forehead or the cheeks where the difference of the density of vertices is large. Vertices with no direct counterparts can be as far as 2 mm from the surface defined by the deformed reference mesh. A good measure of the error introduced during this point correspondence step is the median of the distances, which does not take into account the large distances generated by the lack of correspondence on the boundaries. Upon all samples of the database, the mean median of distances is 0.22 mm (with standard deviation of 0.04 mm). Individual correspondence error range from 0.17 mm to 0.34 mm, whereas the individual mean of the distances range from 0.54 mm to 2.66 mm.

*Figure 3. Establishing correspondences between the face: (a) reference mesh, (b) subject face surface mesh, (c) subject deformed reference mesh*

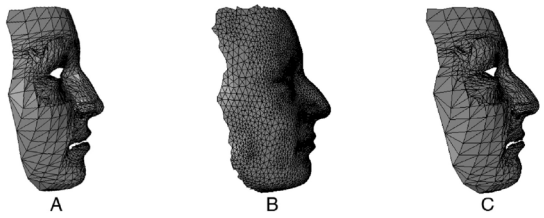


## STATISTICAL METHODS

The variables $\tilde{x}_i$ respectively, $\tilde{y}_i$ are obtained from the positions of the N skull points, respectively L soft-tissue points of subject i:

$$\tilde{x}_i = \left[ S_x^1 S_y^1 S_z^1 \cdots S_x^N S_y^N S_z^N \right] \quad (1)$$

$$\tilde{y}_i = \left[ F_x^1 F_y^1 F_z^1 \cdots F_x^L F_y^L F_z^L \right] \quad (2)$$

Two geometrically averaged templates $\overline{x}$ and $\overline{y}$ are computed and the data are centered:

$$x_i = \tilde{x}_i - \overline{x}_i \quad (3)$$

$$y_i = \tilde{x}_i - \overline{x}_i \quad (4)$$

The data tables *X*, respectively *Y*, of size n x N, respectively n x L, encompass the variables corresponding to the n centered samples $x_i$ and $y_i$ in the learning database. In the following

paragraphs, the transposition of the matrix $X$ will be noted $X^T$ .

## Principal Components Analysis

Principal Components Analysis (Joliff, 1986) performed on the data table $X$ extracts a correlation-ranked set of statistically independent modes of principal variations from the set of subjects described in the data table $X$. These principal modes are vectors of 3D coordinates (of size 3N) defined as linear combinations of point positions. They capture the variations observed over all subjects in the database. The modes are sometimes also called variability parameters. These vectors are the eigenvectors of the covariance matrix $X^T X$ associated to the eigenvalues $l_i$ sorted such as $l_1 > \ldots > l_n \geq 0$. The eigenvectors are orthogonal.

$$l_i a_i = X^T X a_i \,. \tag{5}$$

Every entry $x_i$ in the database can now be represented as a weighted linear combination of these eigenvectors:

$$x_i = \sum c_{ij} a_j \tag{6}$$

where $c_{ij}$ is the weight attached to sample $i$ and eigenvector $j$, also called the principal component of sample $i$ on axis of variability $j$. As the modes are correlation-ranked, the first modes are responsible for the greatest part of the observed variance of the data. In most cases, only a small number of modes is necessary to represent most of the observed data. A classical criterion is to choose the number of modes $t$ in order to represent 95% of the observed variance. A good approximation of each sample is then given using the first t components:

$$x_i = \sum c_{ij} a_j \tag{7}$$

For a new entry $x_0$ , each weight can be extracted as the projection of the sample on each axis of variability:

$$c_{0\mathrm{j}} = x_0^T a_j \tag{8}$$

A new sample can be build from these components and the variability axis.

$$\hat{x}_0 = \sum c_{0\mathrm{j}} a_j$$

A measure of the generalisation power of the model is the reconstruction error, which we will call re-synthesis error to avoid confusion with (facial) reconstruction:

$$E_{0,s} = \left(x_0 - \hat{x}_0\right)^T \left(x_0 - \hat{x}_0\right) \tag{9}$$

which consists in the distance between the re-synthesised sample and the original.

## Principal Components Regressions

Principal Components Regression (PCR) is a linear regression method. The multi-response linear regression model for centred data is defined as:

$$Y = XB + E \tag{10}$$

where $B$ is 3N x 3L matrix of regression coefficients and $E$ is a noise matrix of size n x 3L. The elements of the matrix $E$ are assumed to be normally distributed with mean E[E] =~0 and variance var[E] = S. Given a new sample $x_0$ , an estimate of $y_0$ is:

$$y_0 = B^T x_0 \,. \tag{11}$$

The mean square estimation of the coefficients of *B* is given by

$$\hat{B} = \left(X^T X\right)^{-1} X^T Y \,. \tag{12}$$

However, in case where the predictors (x) present a lot of co-linearity, this estimation is not optimal and a common way is to substitute the predictors by the first t principal components corresponding to the samples of the database, regrouped in matrix *C*. As the axis of variability are orthogonal, there are no co-linearity in the new predictors. A mean square estimation of the regression coefficients between the components *C* and *Y* is build:

$$\hat{G}_{PCR} = \left(C^T C\right)^{-1} C^T Y \tag{13}$$

which can be used to estimate the regression coefficients B, (the matrix *A* regroup the t first axis of variability):

$$\hat{B}_{PCR} = A\left(C^T C\right)^{-1} C^T Y \tag{14}$$

This kind of methods originates from chemiometrics were a small number of predictors must predict a great number of outputs. It is then particularly adapted to the ratio between a small number of skull landmarks and the great number of face points. However, the statistical model presented here will take into account only the skull data (X), and so will the regression model. How can we take into account the observed variability of the known face shapes (Y)?

## A Common Statistical Shape Model

Consider the matrix *Z* formed by merging data tables *X* and *Y* and perform Principal Component Analysis on *Z*. The result of this PCA is still a correlation-ranked set of statistically independent modes of principal variations $d_j$, vectors of size 3(N+L). Each eigenvector $d_i$ with positive eigenvalue obtained by PCA can be decomposed as the juxtaposition of two vectors $d_i = \left[v_i w_i\right]$, with $v_i$ of size 3N and $w_i$ of size 3L. Each part $x_i$ and $y_i$ of entry $z_i$ can be expressed sharing the same weights $b_{ij}$ and the vectors $v_i$ and $w_i$:

$$x_i = \sum b_{ij} v_j \tag{15}$$

$$y_i = \sum b_{ij} w_j \tag{16}$$

For facial reconstruction, we search the best model fit: the instance $z_0 = \left[\hat{x}_0 y_0\right]$ of the model the nearer from the measured skull landmarks $x_0$. As $z_0$ can be represented using the parametric representation of the statistical model as a set of weights $b_{0j}$, the problem is resolved finding successively each weight $b_{0j}$ for which the distance between the measured skull landmarks and the points of the model corresponding to skull landmarks is the smallest:

$$b_{Oj} = argmin_{b_{0j}} \left(b_{Oj} v_j - x_0\right)^T \left(b_{Oj} v_j - x_0\right). \tag{17}$$

The solution is given

$$b_{0j} = \left(\overline{x}_0^T v_j\right) / \left(v_j^T v_j\right) \tag{18}$$

and the facial reconstruction is obtained by:

$$\hat{y}_0 = \overline{y} + \sum b_{0j} w_j \,. \tag{19}$$

## Latent Root Regression

Latent Root Regression (LRR) is a linear regression method. LRR is similar to Principal Compo-

nent Regression (PCR) (and Partial Least Square (PLS) regression), with comparable results in the literature. Single response Latent Root Regression (Hawkins 73, Webster et al. 74) use the same vectors $v_i$ as the common statistical shape model to estimate *B*. As these vectors are not necessary orthogonal, an iterative procedure build upon the first latent variable is necessary as in multi-responsee PLS (PLS2) (see Vigneau & Qannari, 2002 for details) for Multi-Response Latent Root Regression. It results in a sequence of orthogonal vectors $\tilde{v}_i$ which enables us to compute regression coefficients, following the formula:

$$\hat{B}_{LRR} = \sum \tilde{v}_i \left( \tilde{v}_i^T X^T X \tilde{v}_i \right)^{-1} \tilde{v}_i^T X^T Y \qquad (20)$$

## RESULTS

### Validation

The validation of the proposed statistical methods for craniofacial reconstruction is obtained by a leave-one-out cross-validation procedure. Each one in his turn, two couples, left and right, of skull and soft-tissue samples are removed from the database and used as test cases, the remaining entries are used to create the statistical model. The skull points of each couple are used as separate entries for the statistical model. The resulting location of the face points are then compared with their real location. However, the location of the face points is the result of the deformation of a common reference mesh. The distance between the location of each predicted face point and the original soft-tissue surface mesh of the test case -which is a better approximation of the ground truth- can be computed and is a more acurate measure.

### How Many Skull Landmarks?

In order to assess the number of necessary skull landmarks, we can use the hierarchical nature of the extraction procedure presented in section 1.2 and the statistical methods presented in Section 2. Each landmark set of inferior level (containing less landmarks) can be used to predict the position of the landmarks of superior level. If one set can predict the positions of all points of all subjects of the following level with a very good accuracy, then there is no information added by the supplementary points. Therefore, it is not necessary to use more points for the description of the skull shape. However, we can first remark that the answer given by this experiment will be related but different to the answer to a question on the number of necessary skull landmarks to facial reconstruction. A common interrogation will be: is all the information given by the skull shape necessary to predict the shape of the face? Secondly, the techniques described here can be used when the skull is fragmented to predict missing fragments of the skull from the remaining parts.

For each set of landmarks, we build a PCA model. It gives us a linear model of the shape variations, as described by the set of landmarks. This model will be used to predict the position of the supplementary points in upper level sets, using Principal Components Regression. However, we first test the generalisation capacity of these models by projecting the landmarks of a test subject into the model, i.e. extracting its variability parameters, and then re-synthesising the landmarks using these variability parameters. If a model has a good generalisation capacity, then the location of the re-synthesised points will be very close to the location of the points of the test subject. These errors correspond to the accuracy of the prediction by model based upon N0 points of a shape described by N0 points, up to the accuracy of the prediction by model N5 of a N5-shape. These first results are shown in the diagonal of the Table 2.

*Table 2. Accuracy of the prediction of landmarks (mm) (number of variability modes used)*

| Sets of points | N0 (26) | N1 (80) | N2 (278) | N3 (1034) | N4 (3986) | N5 (15650) |
|---|---|---|---|---|---|---|
| N0 | 0,04mm (43) | 0,23mm (37) | 2,55mm (18) | 4,29mm (13) | 4,56mm (10) | 4.58 mm (12) |
| N1 | _ | 0,16mm (43) | 3,09mm (19) | 4,47mm (14) | 4,61mm (10) | 4.58 mm (12) |
| N2 | _ | _ | 0,86mm (92) | 1,44mm (79) | 1,40mm (79) | 4.60 mm (10) |
| N3 | _ | _ | _ | 1,13mm (92) | 1,16mm (92) | 1.17 mm (92) |
| N4 | _ | _ | _ | _ | 1.13mm (92) | 1.60 mm (92) |

Next, we use principal components regression (PCR) to predict the location of the supplementary points. If the prediction of these points is accurate, then the supplementary points do not add any information that can't be extrapolated linearly using the previous set of points. Table 2 presents the mean prediction errors of the points introduced by each successive level of the procedure. For example, the model based on N1 points is used for the prediction of shapes described by N2, N3, N4 and N5 points.

First, the generalisation capacity of the different model as measured by the re-synthesis error decreases as the number of points increases (from 26 to 15650): the ratio between the number of points and subjects becomes unbalanced. For a N0, the model is built on 96 subjects for 3*26=78 coordinates, whereas for N5, the model is build on 92 subjects for 3*15650 coordinates. More subjects are necessary to take into account the variability of the data, as the optimal number of modes corresponds to the maximum number of modes. For N3, N4 and N5, the generalisation capacity of the models is not as good, but there are no significant differences between the errors (1.09 mm vs. 1.13 mm).

We can then observe that the model based on N0 points performs as well as the model based on N1 points, whatever the number of points describing the shape to predict, and uses the same number of principal components, even for shapes described by N1 points. Moreover, models based on N0 and N1 points are not sufficient to model the variability of the shapes of the upper levels, as shown by the large prediction errors. This seems to validate the use of a greater number of points than 100.

The models based on N2 and N3 points perform as well for re-synthesis than for the prediction of the supplementary points. It is particularly true in this experiment for the model based on N3 points, which perform as well on prediction than the models based on N4 and N5 points on re-synthesis (1.16 mm vs. 1.13 mm, 1.17 mm vs. 1.09 mm)). For the prediction of a really great number of points (N5), the model based on N2 points performs the same as the model based on less than a hundred of points.

Given our number of subjects in the database, one thousand points seems to be a sufficient number of points to model the shape of the skull. As such a number of points can't be located manually by an expert without being time consumptive, semi-automatic or fully automatic location methods for the landmarks are therefore necessary.

## Facial Reconstruction: Results

The cross-validation procedure was performed on the available database resulting in 47 successive test cases. As the database is composed of half parts of the bone and skin surface, as much as 92 modes can be used for the prediction of the location of the points of the soft-tissue surface. The other limiting factor of the maximum number of modes is the number of known points per entries. For N0 = 26, the total number of components of the known points is 78 and is inferior to the size of the

*Table 3. Accuracy of the prediction of the semi-landmarks (mm) (number of variability modes used)*

| | PCR | PCA JSSM | LRR |
|---|---|---|---|
| N0 | 3.09 + 0.68 mm (11) | 4,09 +1.28 mm (4) | 3,08 + 0.73 mm (13) |
| N1 | 3.08 + 0.67 mm (18) | 3.93 + 1.12 mm (4) | 3.17 + 0.72 mm (12) |
| N2 | 3.05 + 0.69 mm (19) | 3.87 + 1.05 mm (4) | 3,14 + 0.72 mm (12) |
| N3 | 3.07 + 0.69 mm (19) | 3.69 + 0.94 mm (4) | 3,13 + 0.70 mm (12) |
| N4 | 3.08 + 0.70 mm (19) | 3.36 + 0.87 mm (6) | 3.09 + 0.71 mm (14) |

*Figure 4. Example of facial reconstruction for LRR method. Left: Original face surface Reconstructed face. Right: distance card of the prediction of the left and right halves of the soft tissue surface*

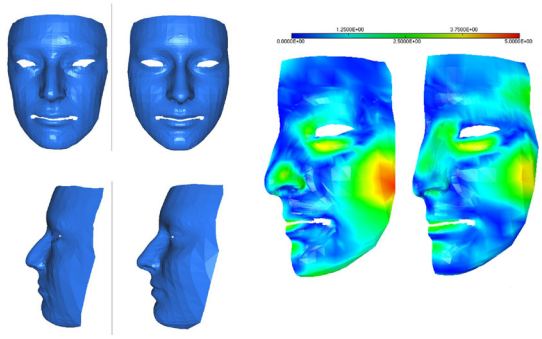

learning base. For the successive level, it won't be an issue as the total numbers of components is 3 times the number of points: the maximum number of modes is the number of learning samples (92).

For the three presented methods, the mean location error is given in Table 2. Figure 4 shows the evolution of the error for the first 25 modes. In a first time, we can observe that proper methods of regression (PCR, LRR) give better results for the task of prediction than the use of a joint statistical shape model. For this method (PCA JSSM), more points correspond to a better prediction of the location of the face semi-landmarks: from a mean prediction error of 4,09 mm with N0 points to a mean prediction error 3.19 mm with N5 points . However, even with N5 points, the prediction error is still higher than for the regression methods: 3.19 mm.

The results given by the regression methods are equivalent between each methods, and the benefits given by the number of points is less observable as the values of the mean prediction error are very close whatever the number of points: between 3.05 mm and 3.17 mm. The results given by the PCR method are consistent with the test realised to decipher the number of skull landmarks, with the best prediction given for N2 (then N3) points. Remember that for N5 points, most of the supplementary points locations can be predicted using N3 points. The number of face points to be predicted (14616) is in the same range than N5, but the relationships between the points are not in these case concerning the interior of a triangle surface patch. For latent root regression, who shares a common scheme with the joint statistical shape model, the more points the more precise the prediction is, except for the N0 shape and N5 shape. N0 is influenced by the good prediction of one of the case, as the standard deviation (0.73mm) for N0 point is higher for any other results.

The results presented here plead for the use of a regression method, but which one choose. PCR performs slightly better than LRR and is less influenced by the number of skull points used in the model. For the moment, it seems that any latent variable linear regression can be chosen without great difference. The ideal number of points is in the range of a thousand.

This mean points location error is very influenced by the point correspondence procedure used for the soft-tissue surfaces. As the objective of facial reconstruction is to provide a prediction of the shape of the soft-tissue surface, a better measure would be the mean distance between the predicted points and the soft-tissue surface reconstructed from the original scan images. Moreover,

*Table 4. Mean points-to-surface error (mm) (number of variability modes used)*

| | PCR | PCA JSSM | LRR |
|---|---|---|---|
| N0 | 1,31+0.28 mm (23) | 1,89+0.50 mm (4) | 1,33 + 0.26 mm (13) |
| N1 | 1,33+0.28 mm (19) | 1,77+0.50 mm (4) | 1,38 + 0.27 mm (13) |
| N2 | 1,30+0.26 mm (17) | 1,74+0.41 mm (4) | 1,36 + 0.25 mm (16) |
| N3 | 1,31+0.26 mm (18) | 1,64+0.37 mm (8) | 1,34 + 0.25 mm (16) |
| N4 | 1,32+0.26mm (17) | 1,48+0.29 mm (9) | 1,33 + 0.24 mm (15) |

*Figure 5. Mean error by points for N0 / LRR (left) and difference in mean error cards for subsequent level of number of points (right)*

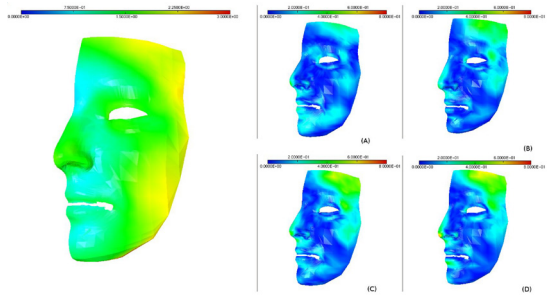

the points-to-surface error is the measure used in most works in facial reconstruction. Table 4 presents the results for the points-to-surface error. The results follow the same pattern than the points-to-points error and with a new order of magnitude of 1.4 mm, slightly modified by the projection operation on the surfaces.

An example of facial reconstruction is presented figure 4 for LRR method, with the associated distance cards. At each face landmark, a colour is associated following the prediction error giving us a spatial map of the reconstruction error. This reconstruction corresponds to the following global errors: 2.50 + 0.87 mm(P-P), 1.06 + 0.84 mm (P-S). The range of prediction error for a point is 0.007 mm to 4,81mm. The highest reconstruction errors are located on the side of the face in the masseter region. The others regions with high errors correspond to the nose and the lower eyelid. Note that the predictions and distance cards for each halve of the face is slightly different, as the face and the skull landmarks are not symmetric. However, each reconstructed half face shares many common features.

For each method, points number and components number, we can compute mean and standard deviation for each predicted point of the mask. The resulting spatial maps of the quality of the reconstruction procedure for the optimal number of parameters can be seen in figure 5 for the local mean. The mean local errors range from 0.75 mm to 3 mm. Whatever the method, the facial areas with the highest reconstruction error are the outer limits of the surface and are for a part an artefact of the point correspondence step: there is no explicit correspondence to fix the limits of the surface in these zones. In the interior part of the face, the region with highest reconstruction error are the masseter region. These regions have few skull landmarks and the bones does not support the soft-tissue for a large part of the cheeks. The regions with the smallest errors (0.75 mm to 1 mm) are concentrated toward the middle of the face, a part where the number of skull landmarks is important and where the inter-subjects correspondence between the face meshes is more constrained. The effect of the increase of the number of skull landmarks can be observed in the difference in the error cards shown in Figure 5. The zones impacted by the increase are the nose and the side of the forehead above the temple.

The mesh-matching algorithm used to provide the point correspondence between the soft-tissue surfaces can be used in a facial reconstruction method by deformation. The deformation field computed between a source skull surface and a destination skull can be applied to the soft-tissue surface of the source. A couple of skull and soft-tissue surfaces can be chosen as the closest skull surface or each surfaces couple of the database

*Table 5. Mean points-to-surface reconstruction error for deformation methods*

| | N0 | N1 | N2 | N3 | N4 |
|---|---|---|---|---|---|
| Mean | 2.61 mm | 2.64 mm | 2.78 mm | 2.86 mm | 2.88 mm |

can be used and every deformed soft-tissue surface computed and considered. On a second time, a mean soft-tissue surface can be computed, merging all the deformed soft-tissue surfaces obtained by computing the mean location of the facial semi-landmarks. The accuracy of the deformation field depends on the number of points, as the criterion behind the computation of the deformation is the distance between the two surfaces.

Table 5 presents the mean points-to-surface error obtained using the different skull shapes for computing the deformation field. As we try to extrapolate the deformations fields for the deformation of the face surfaces, a very precise deformation field is not a benefit as seen with the increase of the error following a large increase in the number of points.

## Comparison with Other Methods

We compare our results to those of Claes (2006) and Vandermeulen (2006). Among reconstruction techniques, the technique described in Claes (2006) is close to ours, with a supplementary deformation phase after the statistical prediction. The statistical step consists in finding the instance of a statistical face model coinciding with "dowels" of tissue thickness placed upon the skull landmarks. It corresponds to the joint statistical model method for a small number of skull landmarks (in the order of N1). The study is conducted on a database of 118 samples. The reconstruction error corresponds roughly to our point-to-surface errors. The mean reconstruction error is 1.14 mm with a standard deviation of 1.04 mm. The highest reconstruction errors (4 mm) are located in the chin and eyes regions, with errors for the region of the cheeks and the nose (except the tip) toward 2 mm. In regard to the smaller database and difference in the points correspondence step and artefacts generated, we seem to be able achieve similar results with a generally simpler methodology, i.e. without supplementary deformation phase with no phisicaly signifiance.

The technique developed in Vandermeulen (2006) is based on the use of continuous surface and the study conducted on 20 samples. The mean reconstruction error is 1.9 mm with a standard deviation of 1.7 mm. The largest reconstruction errors (2-3 mm on average) occurs on the nostrils and masseter region. We appear to outperform those results, however based on a smaller database. We can remark that the regions with large reconstruction errors coincide. Tilotta (2007) propose a local method of facial reconstruction combining prediction obtained on surface patches, delimited by landmarks. The study has been performed on two regions: the nose region and the chin region. For our methodology, the mean reconstruction error for the nose is 1.40 mm with a standard deviation of 0.25 mm. The mean reconstruction for the chin region is of 1.51 mm with 0.67 mm standard deviation. The results presented in this report outperform these estimations with a mean reconstruction error of 0.99 mm, which motivates us to consider more local procedure in the reconstruction process.

## Statistical Shape Models and the Correction of the Shape of the Nose

As seen in the previous section, each of these statistical facial reconstructions are based on statistical shape models, either common or separated. For each model, we can observe the variations of the shape of the face caused by the variations upon each variability modes. For example, figure 6 presents the variations of the face shape according to the 7 first modes of LRR, PCA JSSM and PCR models for parameters of value 3 times standard

*Figure 6. The variations of the face shape according to the 7 first modes of LRR, PCA JSSM and PCR models for parameters of value 3 times standard deviation. Top row: PCR model. Middle row: PCA JSSM model. Bottom row: LRR model*

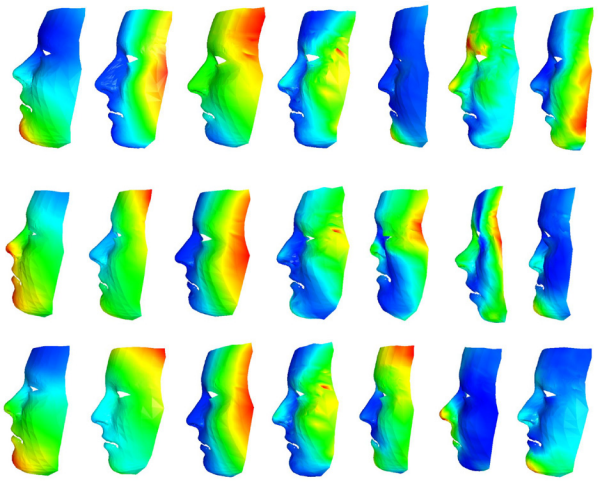

deviation. The strength of the variations is given by the color scheme and enables us to locate the parts of the face associated to each mode. The first parameter acts upon the shape of the lower part of the face, with the shape of the chin as the most influenced part of the face for both regression methods. For LRR and PCA JSSM, the second parameter models the higher part of the face, particularly the outer edge of the mask, whereas the third parameter influences variations of the skull width. For PCR, the second parameter models the difference between compressed and elongated faces along the anterior-posterior axis and these variations corresponds roughly to the third mode of the LRR model, whereas the third is linked to the height of the face. As LRR and PCA JSSM take into account the observed variability of the face points, the second parameter reproduces the large variability of the frontier of the face mask, a variability that cannot be observed in the skull points for the PCR model and thus not taken into account by the PCR model. The fourth parameter concerns the temporal region for all models. Beginning with fifth mode, each part of the model is described differently for each methods.

There are as much parameters than the minimum between the number of subjects or the number of points coordinates. However, as only the first parameters will be selected by the cross-validation procedure, if the parameters acting upon the variation of shape of the nose are later modes, no variation of the shape will be predicted for any test subject. All reconstructed faces will then share the same shape of the nose. Which parameters affect the shape of the nose and which skull landmarks correspond to the prediction of the shape of the nose, can be answered by the observation of the variations of the shape according to the modes. In the LRR case, the first parameter with consequences for the shape of the nose is the 6$^{th}$ parameter. The joint statistical shape model distributes variations on the shape of the nose between the 5$^{th}$ and the 6$^{th}$ parameters. PCR do not present any modes in the twenty first that influences only the shape of the nose.

As we know that our method performs badly for this region, we can offer several predictions with different shapes of nose, corresponding to different values of the “nose” parameters of the model. For example for the reconstructed test

subject presented Figure 3 shows a very different shape of the nose than the original subject. Such modification on the value of a parameter will increase the facial reconstruction error as defined previously, but perhaps offer better recognition chances.

## CONCLUSION

We proposed a statistical method for 3D computerised forensic facial reconstruction. It relies on the use of a common set of points for the description of the individuals. In this set of points, anatomical skull landmarks are completed by points located upon geodesic curbs linking the anatomical landmarks. Facial landmarks are obtained using a mesh-matching algorithm between a common reference mesh and the individual soft-tissue surface meshes. The facial reconstruction problem is resolved by the building of a linear regression model following either Latent Root regression method or Principal Component Regression method for equivalent results. The accuracy of the reconstructions made by the method was measured by leave-one-out cross-validation tests and compared to the use of a joint statistical shape model of both skull and face and a facial reconstruction method based on deformation fields. These results were discussed in regard to the results of other facial reconstruction methods on different databases and in regards to the problem of the shape of the nose. In conjunction, we have addressed the practical problem of the choice of the number of skull landmarks. Depending on the statistical method used and taking into account the size of the database and the limits of the extraction procedure, the necessary number ranges from two hundred to one thousand.

Some extensions can be proposed to the reconstruction method. First of all, having a larger database will increases the flexibility of the model. The more examples of the surfaces the model has, the better the relationships between the two surfaces are learned and the better the models based on a great number of skull landmarks will perform. Secondly, a better control of the point correspondence procedure for the soft-tissue meshes is necessary in order to soften the errors observed in the outer boundaries of the face mask. Then, an automatic extraction of the anatomical landmarks from the skull would make the complete reconstruction pipeline automatic. Lastly, to complete the computer-aided facial reconstruction procedure as a tool of generation of possible faces associated to an unknown skull, some graphic oriented computer applications must be added. A first one is the use of textures for the skin and the integration in the generated meshes of artificial eyes and hairs -which corresponds to the fourth step of reconstruction procedures (Mask Design / Virtual Make-Up). With these added features, a computerised facial reconstruction approach can compete with manual techniques. A second part would be the animation of the face using movements learned on example. The main principles applies for learning the movement of one face and for learning the variability of shapes observed between subjects. Numerous studies and data exist in the field of audiovisual speech (Bailly, 2003; Cohen, 2002; Lee, 1995; Pandzic, 2002; Turakate, 2003), where the main goal is to create "talking heads" of subjects. Other related and collaborative problems for facial reconstruction could also be found in maxillo-facial surgery (Marécaux, 2003; Payan, 2002; Schramm, 2006; Zachow, 2006), where one tries to predict the shape of face following an ablation of the jaw bones.

## REFERENCES

Bailly, G., Bérar, M., Elisei, F., & Odisio, M. (2003). Audiovisual speech synthesis. *International Journal of Speech Technology*, *6*(4), 331–346. doi:10.1023/A:1025700715107

Basso, C., & Vetter, T. (2005). Statistically motivated 3D faces reconstruction . In Buzug, T. M., Sigl, K.-M., Bongartz, J., & Prüfer, K. (Eds.), *Facial reconstruction* (pp. 450–469). München: Wolters/Kluwer.

Berar, M., Desvignes, M., & Bailly, G. (2006). 3D semi-landmarks-based statistical face reconstruction. *Journal of Computing and Information Technology*, *14*(1), 31–43. doi:10.2498/cit.2006.01.04

Bérar, M., Desvignes, M., Bailly, G., & Payan, Y. (2004). *3D meshes registration: Application to statistical skull model* (pp. 100–107). Berlin, Heidelberg: Springer.

Bookstein, F. L. (1997). Landmark methods for forms without landmarks: Morphometrics of group difference in outline shape. *Medical Image Analysis*, *1*, 225–243. doi:10.1016/S1361-8415(97)85012-8

Buzug, T. (2006). Special issue on computer assisted craniofacial reconstruction and modelling [Editorial]. *Journal of Computing and Information Technology*, *14*(1), 1–6. doi:10.2498/cit.2006.01.01

Claes, P., Vandermeulen, D., De Greef, S., Willems, G., & Suetens, P. (2006). Craniofacial reconstruction using a combined statistical model of face shape and soft tissue depths: Methodology and validation. *Forensic Science International*, *159*, 147–158. doi:10.1016/j.forsciint.2006.02.035

Clement, J. G., & Marks, M. K. (2005). *Computer-graphic craniofacial reconstruction*. Boston: Academic Press.

Cohen, M. M., Massaro, D. W., & Clark, R. (2002). Training a talking head. In *Proceedings of IEEE Fourth International Conference on MultiModal Interfaces,* (pp. 499–504).

Cootes, T. F., Taylor, C. J., Cooper, D., & Graham, J. (1995). Active shape models-their training and application. *Computer Vision and Image Understanding*, *61*(1), 38–59. doi:10.1006/cviu.1995.1004

De Greef, S., & Willems, G. (2005). Three-dimensional craniofacial reconstruction in forensic identification: Latest progress and new tendencies in the 21st century. *Forensic Science International*, *50*(1), 12–17.

Evenhouse, R., Rasmussen, M., & Sadler, L. (1992). Computer-aided forensic facial reconstruction. *The Journal of Biocommunication*, *19*(2), 22–28.

Evison, M. P. (1996). Computerized three dimensional facial reconstruction. Retrieved from www.shef.ac.uk/assem/1/evison.html

Frangi, A., Rueckert, D., Schnabel, J., & Niessen, W. (2002). Automatic construction of multiple object three-dimensional statistical shape models: Application to cardiac modeling. *IEEE Transactions on Medical Imaging*, *21*(9), 1151–1166. doi:10.1109/TMI.2002.804426

Gunst, R., Webster, J., & Mason, R. (1976). A comparison of least squares and latent root regression estimator. *Technometrics*, *18*, 75–83. doi:10.2307/1267919

Helmer, R. P., Buzug, T. M., & Hering, P. (2003). Plastic facial reconstruction on the skull-a transition in Germany from a conventional technique to a new one. *Proceedings of the First International Conference on Reconstruction of Soft Facial Parts*. (pp. 75–90). Wiesbaden: Bundeskriminalamt.

Hierl, T., Wollny, G., Peter, F., Scholz, E., Schmidt, J.-G., & Berti, G. (2006). CAD-CAM implants in esthetic and reconstructive craniofacial surgery. *Journal of Computing and Information Technology*, *14*(1), 65–70. doi:10.2498/cit.2006.01.07

Hutton, T. J., Cunningham, S., & Hammond, P. (2000). An evaluation of active shape models for the automatic identification of cephalometric landmarks. *European Journal of Orthodontics*, *22*(5), 499–508. doi:10.1093/ejo/22.5.499

Jolliffe, I. T. (1986). *Principal component analysis*. Berlin: Springer Verlag.

Jones, M.W. (2001). *Facial reconstruction using volumetric data*.

Kähler, K., Haber, J., & Seidel, H.-P. (2003). Reanimating the dead: Reconstruction of expressive faces from skull data. In *ACM Transactions on Graphics (SIGGRAPH 2003 Conference Proceedings), 22*(3), 554–561.

Kermi, A., Bloch, I. & Laskri, M.T. (2007). A non-linear registration method guided by b-splines free-form deformations for three-dimensional facial reconstruction. *International Review on Computers and Software, 20*.

Kuratate, T., Vatikiotis-Bateson, E., & Yehia, H. (2003). Cross-subject face animation driven by facial motion mapping. In Proceedings of *CE2003: Advanced Design, Production, and Managements systems*, (pp. 971–979).

Lee, Y., Terzopoulos, D., & Walters, K. (1995). *Realistic modeling for facial animation* (pp. 55–62).

Mang, A., Müller, J., & Buzug, M. T. (2005). Soft-tissue segmentation in forensic applications . In Buzug, T. M., Sigl, K.-M., Bongartz, J., & Prüfer, K. (Eds.), *Facial reconstruction* (pp. 62–67). München: Wolters/Kluwer.

Mang, A., Müller, J., & Buzug, T. M. (2006). A multi-modality computer-aided framework towards postmortem identification. *Journal of Computing and Information Technology*, *14*(1), 7–19. doi:10.2498/cit.2006.01.02

Marécaux, C., Sidjilani, B. M., Chabanas, M., Chouly, F., Payan, Y., & Boutault, F. (2003). A new 3D cephalometric analysis for planning in computer aided orthognatic surgery. *Computer Aided Surgery*, *8*(4), 217.

Michael, S. D., & Chen, M. (1996). The 3-D reconstruction of facial features using volume distortion. *Proceedings of 14th Annual Conference of Eurographics*, (pp. 297-305).

Nelson, L. A., & Michael, S. D. (1998). The application of volume deformation to three dimensional facial reconstruction: A comparison with previous techniques. *Forensic Science International*, *94*, 167–181. doi:10.1016/S0379-0738(98)00066-8

Pandzic, I. S., & Forchheimer, R. (2002). *MPEG-4 facial animation. The standard, implementation, and applications*. Chichester, UK: John Wiley & Sons. doi:10.1002/0470854626

Payan, Y., Chabanas, M., Pelorson, X., Vilain, C., Levy, P., & Luboz, V. (2002). Biomechanical models to simulate consequences of maxillofacial surgery. *Comptes Rendus Biologies*, *325*, 407–417. doi:10.1016/S1631-0691(02)01443-9

Paysan, P., Luthi, M., Albrecht, T., Lerch, A., Amberg, B., & Santini, F. (2009). Face reconstruction from skull shapes and physical attributes. In . *Proceedings of DAGM-Symposium*, *2009*, 232–241.

Pighin, F., Szeliski, R., & Salesin, D. H. (1999). Resynthesizing facial animation through 3D model-based tracking. In . *Proceedings of International Conference on Computer Vision*, *1*, 143–150. doi:10.1109/ICCV.1999.791210

Quatrehomme, G., Cotin, S., Subsol, G., Delingette, H., Garidel, Y., & Ollier, A. (1997). A fully three-dimensional method for facial reconstruction based on deformable models. *Journal of Forensic Sciences*, *42*(3), 649–652.

Rhine, J. S., & Campell, H. R. (1980). Thickness of facial tissue in American blacks. *Journal of Forensic Sciences*, *25*(4), 847–858.

Rhine, J. S., & Moore, C. E. (1984). *Facial reproduction: Tables of facial tissue thickness of American caucasoids in forensic anthropology. Technical series 1*. Albuquerque: University of New Mexico.

Schramm, A., Schön, R., Rüker, M., Barth, E.-L., Zizelmann, C., & Gellrich, N.-C. (2006). Computer assisted oral and maxillofacial reconstruction. *Journal of Computing and Information Technology*, *14*(1), 71–77. doi:10.2498/cit.2006.01.08

Sethian, J. (1999). *Level sets methods and fast marching methods*. Cambridge University Press.

Shahrom, A. W., Vanezis, P., Chapman, R. C., Gonzales, A., Blenkinsop, C., & Rossi, M. L. (1996). Techniques in facial identification: Computer-aided facial reconstruction using a laser scanner and video superimposition. *International Journal of Legal Medicine*, *108*, 194–200. doi:10.1007/BF01369791

Stratomeier, H., Spee, J., Wittwer-Backofen, U. & Bakker, R. (2005). *Methods of forensic facial reconstruction*.

Surazhsky, V., Surazhsky, T., & Kirsanov, D. (2005). Fast, exact, and approximate geodesics on meshes. In *Proceedings of ACM SIGGRAPH 2005, 24*(3).

Szeliski, R., & Lavallee, S. (1996). Matching 3-D anatomical surfaces with non-rigid deformation using octree splines. *International Journal of Computer Vision*, *18*(2), 171–186. doi:10.1007/BF00055001

Tilotta, F., et al. (2007). Statistical facial reconstruction by tree functional regression on surfaces. *Proceedings of the Third Mediterranean Academy of Forensic Sciences Congress, Porto, Portugal.*

Tilotta, F., Richard, F., Glaunès, J., Bérar, M., Gey, S., & Verdeille, S. (2009). Construction and analysis of a head CT-scan database for craniofacial reconstruction. *Forensic Science International*, *191*(1), 112–118. doi:10.1016/j.forsciint.2009.06.017

Tu, P., Book, R., Liu, X., Krahnstoever, N., Adrian, C., & Williams, P. (2007). Automatic face recognition from skeletal remains. In *IEEE Computer Society Conference on Computer Vision and Pattern Recognition (CVPR 2007)*, Minneapolis.

Vandermeulen, D., Claes, P., Loeckx, D., De Greef, S., Willems, G., & Suetens, P. (2006). Computerized craniofacial reconstruction using CT-derived implicit surface representations. *Forensic Science International*, *159*, S164–S174. doi:10.1016/j.forsciint.2006.02.036

Vanezis, P., Vanezis, M., McCombe, G., & Niblett, T. (2000). Facial reconstruction using 3-D computer graphics. *Forensic Science International*, *108*(2), 81–95. doi:10.1016/S0379-0738(99)00026-2

Vigneau, E., & Qannari, M. (2002). A new algorithm for latent root regression analysis. *Computational Statistics & Data Analysis*, *41*, 231–242. doi:10.1016/S0167-9473(02)00071-3

Wang, Y., Peterson, B., & Staib, L. (2000). Shape-based 3D surface correspondence using geodesics and local geometry. *IEEE Conference on Computer Vision and Pattern Recognition, 2*, 644-651.

Wilkinson, C. (2005). Computerized forensic facial reconstruction: A review of current systems. *Forensic Science, Medicine, and Pathology*, *1*(3), 173–177. doi:10.1385/FSMP:1:3:173

Zachow, S., Hege, H.-C., & Deuflhard, P. (2006). Computer assisted planning in cranio-maxillofacial surgery. *Journal of Computing and Information Technology*, *14*(1), 53–64. doi:10.2498/cit.2006.01.06

## KEY TERMS AND DEFINITIONS

**Landmark:** An anatomical structure used as a point of orientation in locating other structures.

**Regression: A:** functional relationship between two or more correlated variables that is often empirically determined from data and is used especially to predict values of one variable when given values of the others <the regression of *y* on *x* is linear>

**Template:** A template can be thought of as an exemplary instance of the object, containing all the information required to measure and analyze the object. The most common dataset in orthodontics is related to analysis of a lateral cephalogram and contains the conventional cephalometric points and measurements. However, templates are completely user-definable, so they can be created for whatever purpose is desired. Examples include templates for measuring dental casts, facial photographs, osseous structures from CTs, etc.